

Interplay between PIP₃ and calmodulin regulation of olfactory cyclic nucleotide-gated channels

James D. Brady*, Elizabeth D. Rich†, Jeffrey R. Martens‡, Jeffrey W. Karpen§, Michael D. Varnum†, and R. Lane Brown*¶

*Neurological Sciences Institute and §Department of Physiology and Pharmacology, Oregon Health & Science University, Portland, OR 97006; †Department of Veterinary and Comparative Anatomy, Pharmacology, and Physiology, and Program in Neuroscience, Washington State University, Pullman, WA 99164; and ‡Department of Pharmacology, University of Michigan, Ann Arbor, MI 48109

Edited by King-Wai Yau, Johns Hopkins University School of Medicine, Baltimore, MD, and accepted by the Editorial Board August 29, 2006 (received for review April 24, 2006)

Phosphatidylinositol-3,4,5-trisphosphate (PIP₃) has been proposed to modulate the odorant sensitivity of olfactory sensory neurons by inhibiting activation of cyclic nucleotide-gated (CNG) channels in the cilia. When applied to the intracellular face of excised patches, PIP₃ has been shown to inhibit activation of heteromeric olfactory CNG channels, composed of CNGA2, CNGA4, and CNGB1b subunits, and homomeric CNGA2 channels. In contrast, we discovered that channels formed by CNGA3 subunits from cone photoreceptors were unaffected by PIP₃. Using chimeric channels and a deletion mutant, we determined that residues 61–90 within the N terminus of CNGA2 are necessary for PIP₃ regulation, and a biochemical “pull-down” assay suggests that PIP₃ directly binds this region. The N terminus of CNGA2 contains a previously identified calcium–calmodulin (Ca²⁺/CaM)-binding domain (residues 68–81) that mediates Ca²⁺/CaM inhibition of homomeric CNGA2 channels but is functionally silent in heteromeric channels. We discovered, however, that this region is required for PIP₃ regulation of both homomeric and heteromeric channels. Furthermore, PIP₃ occluded the action of Ca²⁺/CaM on both homomeric and heteromeric channels, in part by blocking Ca²⁺/CaM binding. Our results establish the importance of the CNGA2 N terminus for PIP₃ inhibition of olfactory CNG channels and suggest that PIP₃ inhibits channel activation by disrupting an autoexcitatory interaction between the N and C termini of adjacent subunits. By dramatically suppressing channel currents, PIP₃ may generate a shift in odorant sensitivity that does not require prior channel activity.

lipid signaling | olfaction | phosphatidylinositol | sensory adaptation

Odorant binding to specialized receptors in the cilia of olfactory sensory neurons triggers an increase in intracellular cAMP (1–4), which directly opens cyclic nucleotide-gated (CNG) channels (5). Calcium influx through CNG channels activates an atypical chloride current (6–8), leading to depolarization of the cell membrane. The elevated calcium also causes rapid adaptation to odorants by triggering a calcium–calmodulin (Ca²⁺/CaM)-dependent decrease in the sensitivity of CNG channels to cAMP (9). Recent evidence suggests that phosphatidylinositol-3,4,5-trisphosphate (PIP₃) also decreases the sensitivity of olfactory CNG channels and reduces the response of olfactory sensory neurons to complex odors, but the mechanism has yet to be elucidated (10, 11).

Ca²⁺/CaM inhibits homomeric CNGA2 channel activation by binding to a Baa-like motif in the N terminus (12–14), thereby disrupting an autostimulatory interaction with the C terminus of an adjacent subunit (15–17). Deletion of the Ca²⁺/CaM-binding domain (amino acids 68–81) in CNGA2 produces channels that are resistant to inhibition by Ca²⁺/CaM and exhibit dramatically reduced sensitivity to cyclic nucleotides due to the loss of the autostimulatory interaction. Native olfactory CNG channels are tetrameric assemblies of three different pore-forming subunits, CNGA2, CNGA4, and CNGB1b, in a 2:1:1 stoichiometry (18–20). Surprisingly, the N-terminal Ca²⁺/CaM-binding site on CNGA2 is functionally silent in heteromeric channels; instead, Ca²⁺/CaM

exerts its inhibitory effect by binding to IQ-like motifs in the CNGA4 and CNGB1b subunits (21).

More recently, several lipids have been shown to regulate the activity of CNG channels. Activation of rod channels is reduced dramatically by application of diacylglycerol derivatives (22, 23), *all-trans*-retinal (24), and phosphatidylinositol-4,5-bisphosphate (PIP₂) (25), and activation of olfactory CNG channels is inhibited by cholesterol depletion (26). Zhainazarov *et al.* (11) reported that PIP₃ inhibits heterologously expressed CNGA2 homomeric channels or CNGA2/CNGA4 heteromeric channels to nearly the same extent as native channels in olfactory sensory neuron membranes. Interestingly, inhibition by PIP₃ in many respects resembles that of Ca²⁺/CaM: in both cases, the apparent affinity of the channel for cAMP is reduced by at least 10-fold with no change in the single-channel conductance. Whereas the mechanism of Ca²⁺/CaM inhibition has been well characterized, the molecular mechanisms underlying PIP₃ inhibition remain unknown. Furthermore, it is unclear how these two regulatory processes interact to modulate the odorant response.

Results

CNGA3 Channels Are Insensitive to PIP₃. To investigate the effects of PIP₃ on CNG channel function, we expressed cloned channel subunits in HEK293 cells and exposed inside-out patches to varying concentrations of cyclic nucleotides. As shown in Fig. 1 *A* and *D*, exposure of patches containing homomeric CNGA2 channels to 10 μM dipalmitoyl-PIP₃ produced, on average, a 17- and 13-fold shift in the apparent affinity for cGMP ($n = 8$) and cAMP ($n = 12$), respectively. In addition, dipalmitoyl-PIP₃ (hereafter referred to as PIP₃) decreased the efficacy of saturating cAMP by ≈70%, an effect typically ascribed to stabilization of closed-channel states. The decrease in cyclic nucleotide sensitivity generally occurred within 20 seconds of exposure to 10 μM PIP₃; similar results were observed with concentrations of PIP₃ as low as 1 μM, but the time course was generally slower (Fig. 1 *C*). We were unable to reverse the effect of PIP₃, even with wash times of >60 min, which we attribute to the high affinity of PIP₃ for the hydrophobic membrane environment. Application of 50 μM dioctanoyl-PIP₃ (a more water soluble analog with shorter acyl substituents) caused only a mild decrease in the apparent cAMP affinity (<2-fold), whereas 10 μM dioctanoyl-PIP₃ and 10 μM IP₄ had no effect (data not shown). In approximately half of the patches, PIP₃ reduced the saturating

Author contributions: J.D.B., J.W.K., M.D.V., and R.L.B. designed research; J.D.B. and E.D.R. performed research; J.D.B., M.D.V., and R.L.B. analyzed data; and J.D.B., J.R.M., J.W.K., M.D.V., and R.L.B. wrote the paper.

The authors declare no conflict of interest.

This article is a PNAS direct submission. K.-W.Y. is a guest editor invited by the Editorial Board.

Abbreviations: CNG, cyclic nucleotide-gated; PIP₂, phosphatidylinositol-4,5-bisphosphate; PIP₃, phosphatidylinositol-3,4,5-trisphosphate; Ca²⁺/CaM, calcium–calmodulin.

¶To whom correspondence should be addressed. E-mail: brownla@ohsu.edu.

© 2006 by The National Academy of Sciences of the USA

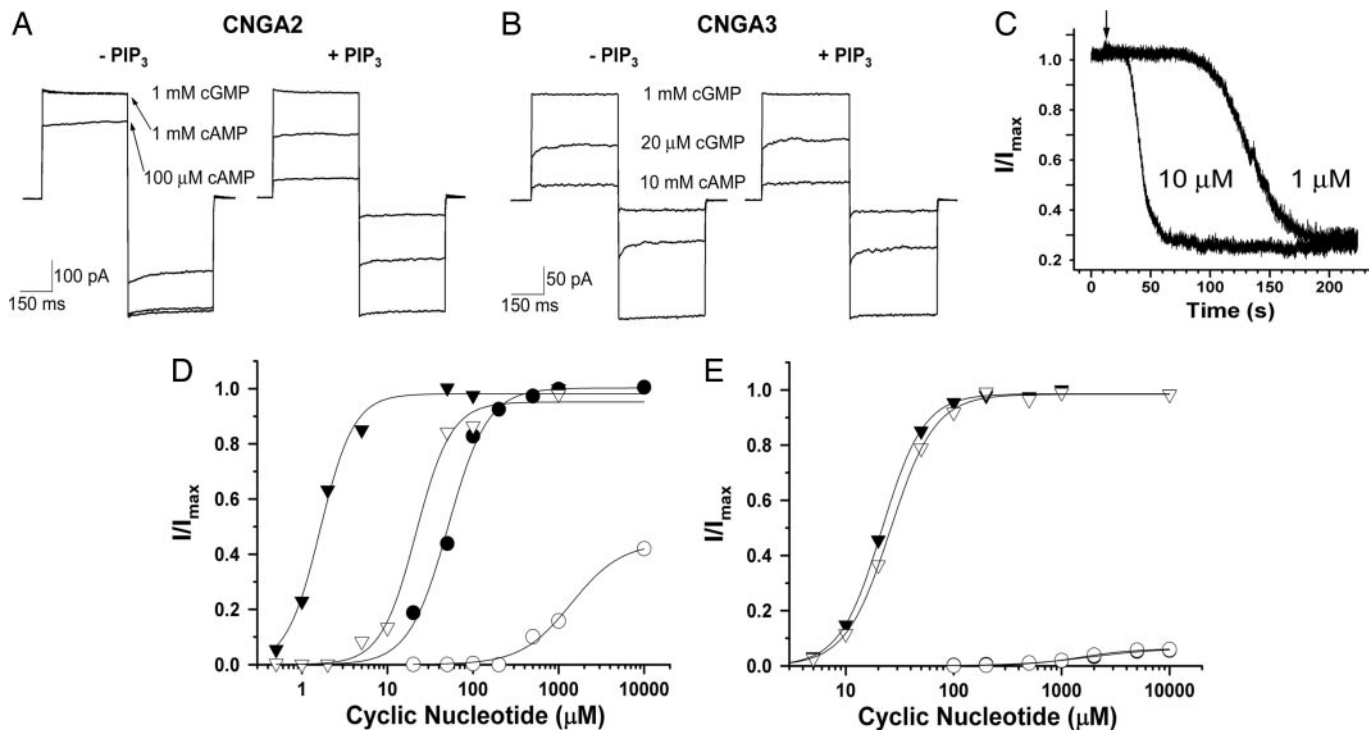


Fig. 1. PIP₃ inhibits CNGA2 channels but not CNGA3 channels. Representative traces from CNGA2 (*A*) and CNGA3 (*B*) before and after application of 10 μ M PIP₃. Currents were elicited by voltage steps to +50 and -50 mV in the presence of the indicated concentration of cyclic nucleotides. Data are representative of 12 patches for CNGA2 and 6 patches for CNGA3. (*C*) Two different patches containing CNGA2 channels activated by 1 mM cAMP and held at -50 mV were exposed to 10 μ M or 1 μ M PIP₃ at 15 s (denoted by arrow). Data were normalized to the current level before PIP₃ exposure. Representative CNGA2 (*D*) and CNGA3 (*E*) cyclic nucleotide dose-response relationships before (filled symbols) and after (open symbols) application of 10 μ M PIP₃. Hill parameters ($K_{1/2}$, n) for CNGA2: (\blacktriangledown) cGMP = 1.6 μ M, 2.2 before PIP₃, and (∇) 21.5 μ M, 2.1 after PIP₃; (\bullet) cAMP = 51.2 μ M, 1.9 before PIP₃, and (\circ) 1.4 mM, 1.5 after PIP₃; for CNGA3: (\blacktriangledown) cGMP = 21.6 μ M, 2.2 before PIP₃, and (∇) 25.8 μ M, 2.1 after PIP₃; (\bullet) cAMP = 1.8 mM, 1.3 before PIP₃, and (\circ) 1.5 mM, 1.7 after PIP₃. Open circles in *E* overlap and hide the filled circles. Data are representative of three separate experiments each for CNGA2 and CNGA3.

cGMP current by 20–30%. This effect developed gradually with prolonged exposure to PIP₃, suggesting that high concentrations of patch-resident PIP₃ were required. We found no correlation between the size of the apparent affinity shift and the decrease in the maximum cGMP-activated current.

In contrast, application of 10 μ M PIP₃ had no effect on channels formed by CNGA3, the α subunit from cone photoreceptors (Fig. 1 *B* and *E*). Neither the apparent affinity for cGMP nor the maximum current elicited by saturating cGMP concentrations was altered significantly by even prolonged exposure to 10 μ M PIP₃ (up to 4 min). Similarly, the apparent affinity and efficacy of cAMP, a weak partial agonist for CNGA3, also were unaffected.

Molecular Determinants of PIP₃ Regulation. To identify channel regions involved in PIP₃ regulation, we constructed chimeric channels by exchanging different regions of CNGA2 and CNGA3. These two subunits are \approx 60% identical and 75% homologous, with most of their differences lying in the cytoplasmic N and C termini. Exchanging the pore domain and C terminus did not eliminate the PIP₃ sensitivity of the parent channel; CNGA2 containing the CNGA3 pore and cyclic nucleotide-binding (CNB) domain (chimera 2233) still was inhibited by PIP₃ (by \approx 5-fold), and CNGA3 channels containing the CNGA2 pore and CNB domain (chimera 3322) were unaffected by PIP₃ (Fig. 24). We then assessed the PIP₃ sensitivity of chimeric channels containing only the cytoplasmic N terminus of CNGA2, and we found that transplantation of this region onto CNGA3 was sufficient to confer PIP₃ inhibition. Exposure of patches containing these chimeric channels (A2nA3) to 10 μ M PIP₃ caused a 5-fold decrease in their cGMP sensitivity,

and a severe reduction in the current elicited by saturating cAMP (Fig. 2).

Calmodulin inhibition of CNGA2 channels resembles PIP₃ inhibition and also relies on residues within the N terminus (residues 68–81). We therefore hypothesized that the two modulators share a common inhibitory mechanism or binding site. In support of this idea, we found that channels formed by CNGA2 subunits lacking residues 61–90 (Δ 61–90-CNGA2) were virtually unaffected by application of 10 μ M PIP₃ (Fig. 34). However, with prolonged PIP₃ exposure, these channels, like WT CNGA2 channels, often exhibited a reduction in the maximum cGMP-activated current but no change in the maximum cAMP-activated current. Although difficult to explain based on current models of CNG channel activation, this effect was not investigated further.

Several mechanistic scenarios might explain the loss of PIP₃ sensitivity in the Δ 61–90-CNGA2 channels. First, PIP₃ might interact directly with amino acids within this region. Alternatively, PIP₃ might bind to adjacent sites and inhibit channels by disrupting the autostimulatory interaction between the N and C termini, which is already absent in the deletion mutant. To test for a direct interaction between PIP₃ and the N terminus of CNGA2, we incubated a GST-tagged peptide containing the cytoplasmic N terminus of CNGA2 (GST-A2N) with PIP₃-conjugated beads. The beads and bound protein were recovered by centrifugation and washed to reduce nonspecific binding. As shown in Fig. 3B, GST alone did not adhere to the PIP₃ beads, but the high-affinity PIP₃-binding domain from Grp1 (GST-Grp1PH) was enriched by the PIP₃ beads. A fraction of the GST-A2N peptide also was recovered with the PIP₃-conjugated beads. In contrast, a CNGA2 N-terminal peptide lacking resi-

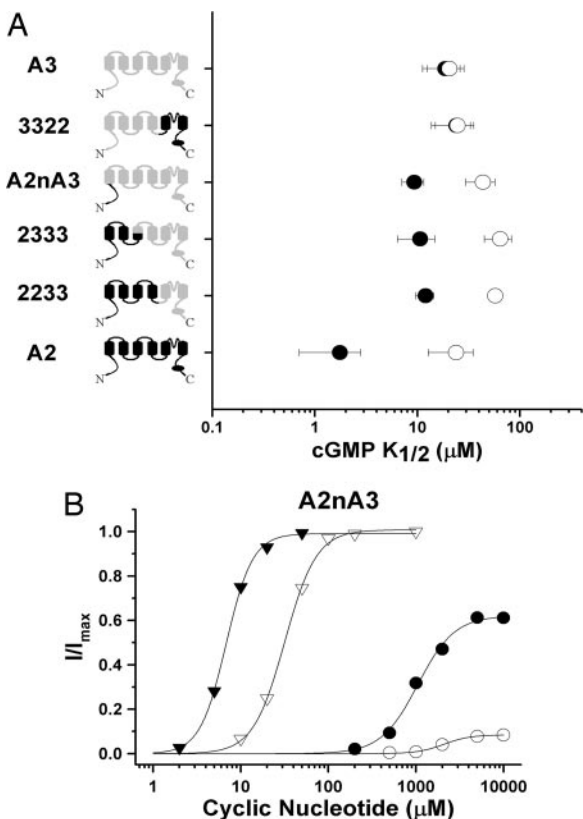


Fig. 2. The N terminus of CNGA2 confers PIP₃ sensitivity to CNGA3 channels. (A) Diagrams depicting CNGA2/CNGA3 chimeric subunits are shown on the left (see *Methods* for splice site locations). Portions of the channel sequence derived from CNGA2 are shown in black; portions derived from CNGA3 are shown in gray. Plotted adjacent is the mean $K_{1/2}$ for cGMP before (●) and after (○) $10 \mu\text{M}$ PIP₃. $K_{1/2}$ values \pm SD are as follows: A3, $18.6 \pm 7 \mu\text{M}$ before PIP₃ and $20.5 \pm 8 \mu\text{M}$ after PIP₃, three patches; 3322, $24.0 \pm 9 \mu\text{M}$ before PIP₃ and $24.6 \pm 11 \mu\text{M}$ after PIP₃, three patches; A2nA3, $9.3 \pm 2.3 \mu\text{M}$ before and $43.5 \pm 13.8 \mu\text{M}$ after, five patches; 2333, $10.6 \pm 4 \mu\text{M}$ before and $64 \pm 19 \mu\text{M}$ after, four patches; 2233, $12.0 \pm 2.4 \mu\text{M}$ before and $57.3 \pm 7 \mu\text{M}$ after, three patches; CNGA2, $1.8 \pm 1 \mu\text{M}$ before and $23.9 \pm 11 \mu\text{M}$ after, nine patches. (B) Representative cyclic nucleotide dose–response relationships, before (filled symbols) and after (open symbols) application of $10 \mu\text{M}$ PIP₃, for channels containing A2nA3 subunits. Hill equation parameters ($K_{1/2}$, n): (▼), cGMP = $6.8 \mu\text{M}$, 2.1 before PIP₃ and (▽) $31.8 \mu\text{M}$, 2.4 after PIP₃; (●), cAMP = 1.0 mM , 2.1 before PIP₃ and (○) $K_{1/2}$ = 2.1 mM , 2.9 after PIP₃. Data are representative of four different patches.

dues 61–90 (GST-A2N Δ) did not adhere to the PIP₃-coated beads. This biochemical result suggests that PIP₃ directly binds to residues in the region between amino acids 61 and 90. Surprisingly, we found that the CNGA3 N terminus also adhered to PIP₃-coated beads (Fig. 3B), even though PIP₃ does not alter CNGA3 channel activity. When the Ca²⁺-CaM-binding site was removed from the CNGA3 N-terminal peptide (GST-A3N Δ), binding to PIP₃ beads no longer was observed. Interestingly, previous biochemical experiments have established that the N terminus of CNGA3 binds Ca²⁺/CaM, but this binding is functionally silent (27).

Native-type olfactory CNG channels, formed by CNGA2, CNGA4, and CNGB1b subunits, were also strongly inhibited by PIP₃. Heteromeric channels containing WT CNGA2 subunits exhibited a 5-fold average increase in their $K_{1/2}$ for cGMP from $2.6 \pm 0.6 \mu\text{M}$ to $15.7 \pm 7.1 \mu\text{M}$ after brief exposures to $10 \mu\text{M}$ PIP₃ (five patches; Fig. 3C). To test the functional relevance of the CNGA2 N-terminal PIP₃-binding site in the context of the heteromeric channel, we expressed the $\Delta 61$ –90-CNGA2 sub-

units along with CNGA4 and CNGB1b. We found that exposure to $10 \mu\text{M}$ PIP₃ had no appreciable effect on the apparent cGMP affinity of these channels ($K_{1/2}$ before PIP₃, $14.7 \pm 3.1 \mu\text{M}$; $K_{1/2}$ after, $19.9 \pm 9.1 \mu\text{M}$, three patches; Fig. 3D). Similar results were observed with cAMP for both WT and mutant channels (Fig. 3C and D). These observations demonstrate that residues 61–90 of CNGA2 are necessary for PIP₃ regulation of heteromeric olfactory CNG channels.

Interplay Between PIP₃ and Ca²⁺/CaM Regulation. Because our biochemical data imply that the PIP₃-binding site overlaps that of Ca²⁺/CaM on CNGA2, we predicted that PIP₃ might occlude the action of Ca²⁺/CaM on homomeric CNGA2 channels. As shown in Fig. 4A, CNGA2 channels exhibited a reversible decrease in their apparent affinity for cGMP after exposure to 250 nM Ca²⁺/CaM ($K_{1/2}$ before Ca²⁺/CaM, $2.3 \pm 1.2 \mu\text{M}$; after Ca²⁺/CaM, $19.2 \pm 5.3 \mu\text{M}$; after EDTA wash, $1.6 \pm 0.4 \mu\text{M}$; four patches). Subsequently, a brief exposure to $10 \mu\text{M}$ PIP₃ inhibited channel activation to an equal, or greater, extent ($K_{1/2}$ = $29.9 \pm 11.4 \mu\text{M}$, four patches). Thereafter, a second exposure to Ca²⁺/CaM produced no further decrease in apparent affinity ($K_{1/2}$ = $29.6 \pm 14.7 \mu\text{M}$, four patches). This finding suggests that PIP₃ and Ca²⁺/CaM exert their effects through a common mechanism or that PIP₃ inhibits Ca²⁺/CaM binding. To test the latter hypothesis, we measured Ca²⁺/CaM binding to the CNGA2 N terminus by using a calmodulin overlay assay (Fig. 4D). We found that the presence of $100 \mu\text{M}$ PIP₃ reduced the binding of FLAG-tagged Ca²⁺/CaM to a GST-tagged CNGA2 N-terminal peptide by almost 70% under our assay conditions ($67.3 \pm 0.06\%$; $n = 6$). Thus, PIP₃ appears to mimic and occlude Ca²⁺/CaM inhibition of homomeric CNGA2 channels, in part, by interfering with Ca²⁺/CaM binding to the CNGA2 N terminus.

In heteromeric olfactory channels, the CNGA2 N-terminal CaM-binding site is functionally silent; instead, Ca²⁺/CaM exerts its inhibitory effects by binding to IQ-like motifs in the CNGA4 and CNGB1b subunits. Therefore, we expected that PIP₃ and Ca²⁺/CaM inhibition would be additive. Surprisingly, we found that WT heteromeric channels were unaffected by application of Ca²⁺/CaM after exposure to $10 \mu\text{M}$ PIP₃ (Fig. 4B). Exposure of heteromeric channels containing $\Delta 61$ –90-CNGA2 to $10 \mu\text{M}$ PIP₃ also occluded inhibition by Ca²⁺/CaM (Fig. 4C), even though PIP₃ had no direct effect on the apparent affinity of the channels. Using calmodulin overlay assays (Fig. 4D), we found that the presence of $100 \mu\text{M}$ PIP₃ inhibited the binding of FLAG-tagged calmodulin to peptides containing the IQ motifs from CNGA4 ($86.1 \pm 0.06\%$; $n = 9$) and CNGB1b ($87.4 \pm 0.08\%$; $n = 7$).

Discussion

We have shown that PIP₃ dramatically shifts the cyclic nucleotide sensitivity of olfactory CNG channels by direct interaction with residues in the N terminus of CNGA2. This interaction mimics and occludes Ca²⁺/CaM regulation in homomeric CNGA2 channels. In heteromeric channels containing CNGA2, CNGA4, and CNGB1b, PIP₃ and Ca²⁺/CaM produce distinct functional changes by binding to different subunits, yet PIP₃ still blocks Ca²⁺/CaM regulation. Our findings reaffirm the regulatory significance of the CNGA2 N terminus in the heteromeric channel and indicate that each subunit in native olfactory CNG channels has a distinct and important role in channel regulation and trafficking (28–30).

Based on our observations, a possible mechanism for PIP₃ inhibition of olfactory CNG channels can be inferred. In homomeric CNGA2 channels, removal of residues 61–90, exposure to Ca²⁺/CaM, and exposure to PIP₃ produce nearly identical shifts in cyclic nucleotide sensitivity and in the maximum cAMP-activated current. The removal of residues 61–90 and regulation

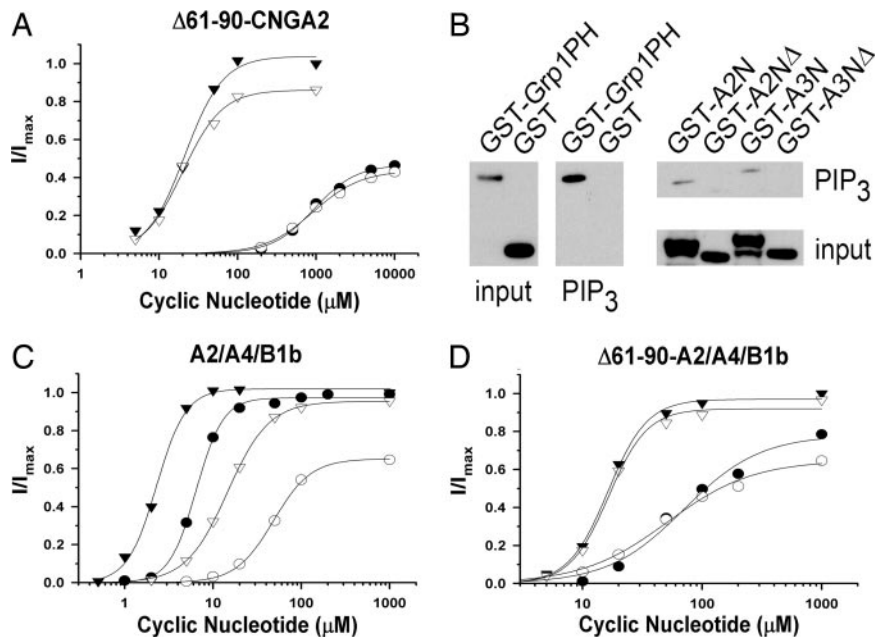


Fig. 3. PIP₃ inhibits olfactory CNG channels through a direct interaction with the N terminus of CNGA2. (A) Shown are representative cyclic nucleotide dose–response relationships for $\Delta 61$ –90-CNGA2, measured before (filled symbols) and after (open symbols) treatment with 10 μ M PIP₃. Hill equation parameters ($K_{1/2}$, n): (▼) cGMP 22.6 μ M, 2.8 before PIP₃ and (▽) 26.9 μ M, 2.2 after PIP₃; (●) cAMP = 1.2 mM, 1.4 before PIP₃ and (○) 917 μ M, 1.6 after PIP₃. Data are representative of three different experiments. (B) N-terminal regions of CNGA2 and CNGA3 were expressed as GST-fusion proteins and tested for PIP₃ binding *in vitro* by using PIP₃-agarose beads. Input proteins (Left and Right Lower) and bound proteins (Middle and Right Upper) were identified by immunoblotting with anti-GST antibodies. GST-Grp1PH, positive control pleckstrin homology domain (Echelon); GST-A2N, N-terminal cytoplasmic domain (amino acids 1–138) of rat CNGA2 (AF126808); GST-A2N Δ , amino acids 61–90 deleted; GST-A3N, N-terminal cytoplasmic domain (amino acids 1–164) of human CNGA3 (AF065314); GST-A3N Δ , amino acids 51–108 deleted. Data are representative of four different experiments. (C) Representative cGMP dose–response relationships before (filled symbols) and after (open symbols) application of 10 μ M PIP₃ to a patch containing wtCNGA2/A4/B1b channels. Hill equation parameters ($K_{1/2}$, n): (▼) cGMP, 2.3 μ M, 2.6 before PIP₃ and (▽) 14.6 μ M, 1.8 after PIP₃; (●) cAMP, 6.4 μ M, 2.8 before PIP₃ and (○) 48.4 μ M, 2.0 after PIP₃. (D) Representative cGMP dose–response relationships before and after application of 10 μ M PIP₃ to a patch containing $\Delta 61$ –90-CNGA2/A4/B1b channels. Hill equation parameters ($K_{1/2}$, n): (▼) cGMP, 16.3 μ M, 2.6 before PIP₃ and (▽) 16.5 μ M, 2.7 after PIP₃; (●) cAMP, 70.4 μ M, 1.4 before PIP₃ and (○) 51.4 μ M, 1.2 after PIP₃. Data are representative of five patches for WT channels and three patches for deletion mutants.

by Ca²⁺/CaM both are known to disrupt an autostimulatory interaction between the N and C termini of adjacent CNGA2 subunits (15, 17). Because PIP₃ inhibition requires residues 61–90 and prevents Ca²⁺/CaM regulation, we postulate that PIP₃ binding may anchor the N terminus of CNGA2 to the membrane surface, thereby disrupting the intersubunit autostimulatory interaction. This molecular mechanism resembles that recently proposed for prevention of K⁺ channel N-type inactivation by phosphoinositides: sequestering of the N-terminal domain at the cytoplasmic face of the membrane (31). Although the N terminus of CNGA3 can bind both PIP₃ and Ca²⁺/CaM, these interactions appear to be functionally silent, most likely reflecting the absence of a pronounced autostimulatory interaction with the C terminus (27). Our data also suggest a possible mechanism for PIP₃ inhibition of heteromeric olfactory channels. As we and others have observed, PIP₃ inhibition of heteromeric channels causes a 10-fold shift in cyclic nucleotide sensitivity and a 2-fold reduction in the efficacy of cAMP (11). In contrast, Ca²⁺/CaM produces a larger shift in cyclic nucleotide sensitivity without decreasing the efficacy of cAMP (12). Taken together, the results suggest that autostimulatory subunit interactions still occur in heteromeric channels, and that PIP₃ inhibits the heteromeric channel by interaction with CNGA2, whereas Ca²⁺/CaM inhibition requires interaction with CNGA4 or CNGB1b (21).

Phosphatidylinositides are known to regulate the activity of an ever-increasing number of ion channels. Binding of PIP₂ to both K_{ir}1 and K_{ir}6 channels promotes channel activation by stabilizing the open state (32–34), and PIP₃ has been proposed to activate both epithelial sodium channels and TRPC6 channels by direct

binding (35, 36). Like PIP₂-binding regions identified in other ion channels (37–39), the stretch of amino acids between residues 61–90 of CNGA2 contains multiple basic residues that may be important for the interaction with negatively charged phospholipids. Similar to PIP₂ inhibition of TRPV1 channels (40), PIP₃ inhibited activation of olfactory CNG channels. PIP₂ and Ca²⁺/CaM have been shown to bind competitively and have antagonistic effects on the activity of many proteins, like RGS4 and MARCKS (41, 42). In contrast, PIP₃ partially mimics and occludes Ca²⁺/CaM regulation of olfactory CNG channels. Our data suggest that for both homomeric and heteromeric olfactory CNG channels, PIP₃ interferes with Ca²⁺/CaM binding to several channel subunits. Additionally, in homomeric channels, binding of PIP₃ may induce a separation of the N and C termini, thereby preventing Ca²⁺/CaM from having any further effect on channel function.

Olfactory sensory adaptation is mediated by Ca²⁺/CaM-dependent channel inhibition and depends on activation of the odorant signaling pathway and the subsequent influx of Ca²⁺ through open CNG channels (9). In contrast, inhibition of olfactory signaling by PIP₃ does not require prior channel activity, and channel regulation by PIP₃ may serve to reduce overall olfactory sensitivity in the presence of complex odorant mixtures. One possible route for PIP₃ synthesis is suggested by the recent discovery of purinergic receptors in olfactory sensory neuron membranes (43). These G protein-coupled receptors are activated by ATP and have been reported to stimulate PIP₃ synthesis in astrocytes and C6 glioma cells (44, 45). In the olfactory epithelium, noxious stimuli or prolonged exposure to odorants may lead to the release of cellular ATP, causing activation of purinergic receptors and consequent

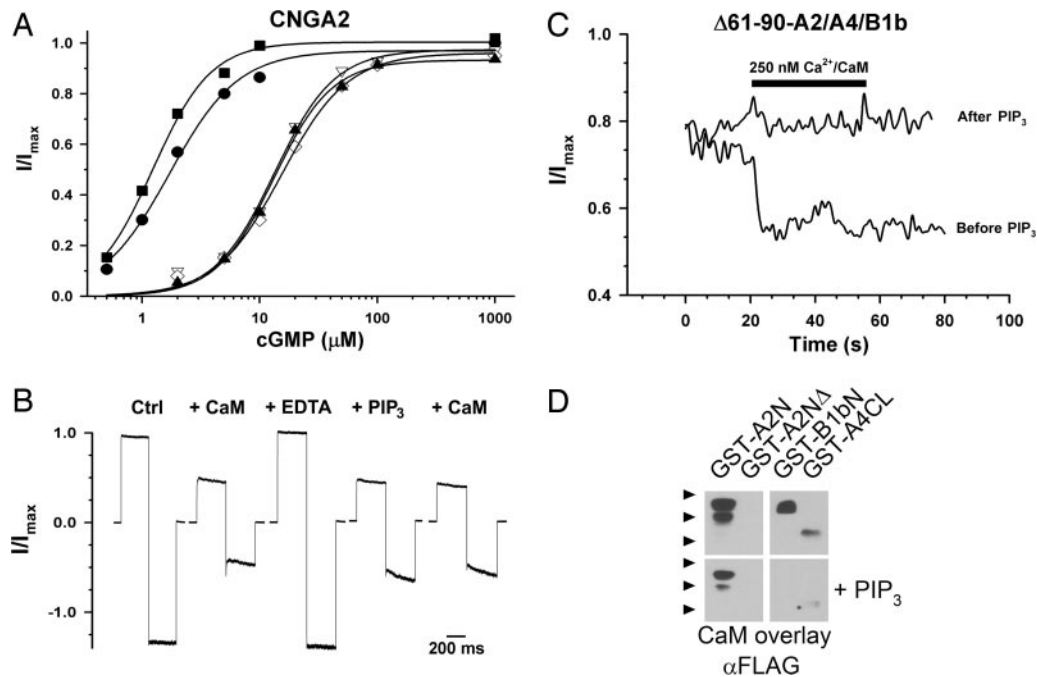


Fig. 4. PIP₃ prevents calmodulin regulation of olfactory CNG channels. (A) CNGA2 cGMP dose–response relationships were measured before (●) and after (▽) application of 250 nM Ca²⁺/CaM. The patch then was washed with 0.5 mM EDTA (■) to remove the CaM. A 10 μM concentration of PIP₃ (◇) caused a right shift that occluded a response to subsequent application of CaM (▲). *K*_{1/2} values: before CaM, 1.7 μM; after CaM, 13.3 μM; EDTA wash, 1.2 μM; after PIP₃, 15.3 μM; PIP₃ + CaM, 13.2 μM. Data are representative of four separate experiments. (B) Representative traces from an inside-out patch containing wtCNGA2/A4/B1b channels stepped to +50 mV and –50 mV and exposed to solutions containing either 500 nM Ca²⁺/CaM or 10 μM PIP₃. Data are representative of three separate experiments. (C) Representative trace from an inside-out patch containing Δ61–90-CNGA2/A4/B1b channels before and after exposure to 10 μM PIP₃. The current activated by 50 μM cGMP was measured at +50 mV every second and normalized to the current activated by 1 mM cGMP. Ca²⁺/CaM (250 nM) was added at 20 s. Data are representative of three separate experiments. (D) After blotting, GST-fusion proteins were probed in an overlay assay by using ≈50 nM FLAG-tagged CaM in 10 μM buffered calcium, either in the presence (below) or in the absence (above) of 100 μM PIP₃. GST-A2N and GST-A2NΔ are as in Fig. 3B; GST-B1bN, proximal N-terminal region (amino acids 677–764) of bovine CNGB1; GST-A4CL, C-linker region (amino acids 271–339) of rat CNGA4. Bound CaM-FLAG was detected by using M2 anti-FLAG antibody. Arrowheads indicate approximate location of molecular mass markers: 49, 38, and 28 kDa. Corresponding blots above and below each other represent identical exposure times. Data are representative of six different experiments.

production of PIP₃. We speculate, therefore, that the stimulation of PIP₃ synthesis by purinergic receptor activation may serve a neuroprotective role by preventing possibly toxic levels of calcium influx through CNG channels after excessive or noxious stimulation.

Materials and Methods

DNA and Mutagenesis. WT bovine CNGA3, rat CNGA2, rat CNGA4, and rat CNGB1b, including the 5′ and 3′ untranslated regions, and all chimeras, were cloned into pcDNA3.0 (Invitrogen, Carlsbad, CA). A YFP-tagged CNGA2 was used (pEYFP-C1; Clontech, Mountain View, CA) and was indistinguishable from the native subunit. Construction of chimeric subunits has been described previously, with splice sites after S229 and I277 in CNGA2 and after V276 and I322 in CNGA3 (46). The A2nA3 chimera was constructed by using overlapping PCR, with residues 1–140 of CNGA2 spliced to residues 186–706 of CNGA3. DNAs encoding the N-terminal regions of rat CNGA2 (residues 1–138) and human CNGA3 (residues 1–164) were genetically fused with DNA-encoding GST (GE Healthcare Biosciences, Piscataway, NJ) as described in refs. 15 and 47. DNAs encoding the proximal N-terminal region of bovine CNGB1b (amino acids 677–764) and the C-linker region of rat CNGA4 (amino acids 271–339) were fused to GST to form CNGB1bN and GST-A4CL.

Cell Culture and Transfection. HEK293 cells were maintained in DMEM (cellgro; Mediatech, Herndon, VA) containing 10% FBS (BioWhittaker Cambrex, East Rutherford, NJ) and 1% Pen-Strep (GIBCO Invitrogen, Carlsbad, CA), at 37°C in a

humidified 95% O₂/5% CO₂ atmosphere. Cells were transfected with FuGENE 6 (Roche, Basel, Switzerland) or Effectene (Qiagen, Valencia, CA) according to the manufacturer’s instructions. An unmodified pEGFP-N2 vector was cotransfected for identification during patch clamping.

Patch-Clamp Analysis. HEK293 cells were lifted into room temperature normal media 18–72 h after transfection and were used for recording within 6 h. Cell aliquots were added to a bath solution containing 130 mM NaCl, 5 mM KCl, 20 mM Hepes, 0.5 mM EDTA, 5 mM MgCl₂, and 2 mM CaCl₂, pH 7.4. Pipettes were filled with a solution matching that in the bath, without MgCl₂ and CaCl₂, and had resistances ranging from 1.5 to 4.0 MΩ. After the formation of a GΩ seal, inside-out patches were excised and placed in front of a perfusion head controlled by a Biologic RSC-100 rapid solution changer (Molecular Kinetics, Pullman, WA). Patches were first washed in a solution containing 130 mM KCl, 5 mM NaCl, 20 mM Hepes, 0.5 mM EDTA (pH 7.4), and then exposed to varying concentrations of cAMP and cGMP (Sigma, St. Louis, MO) dissolved in the perfusion solution. Dose–response curves were generated by subtracting the current recorded at +50 mV in cyclic nucleotide-free solution from the current recorded in the presence of cyclic nucleotide at the same voltage. The leak-subtracted currents were normalized to the current elicited by 1 mM cGMP. Curves are fits to the Hill equation, $I/I_{\max} = C^n/[C^n + (K_{1/2})^n]$, where *C* is the cyclic nucleotide concentration and *n* is the Hill coefficient. For Ca²⁺/CaM experiments, perfusion solutions typically contained 250 nM bovine brain calmodulin (Sigma), 2 mM NTA instead of

EDTA, and 704 μM total CaCl_2 (50 μM free Ca^{2+}). All phosphatidylinositides were obtained from Matreya (Pleasant Gap, PA) as sodium salts and reconstituted with water to stock concentrations of 100 μM . The stock solutions were sonicated at low power for 30 min on ice and stored at -20°C . Perfusion solutions containing phosphatidylinositides were sonicated for an additional 30 min before use. Recordings were made with a CV201 headstage attached to an Axopatch 200A amplifier and a Digidata 1200 interface (Molecular Devices, Sunnyvale, CA). Currents were sampled at 10 kHz and digitally filtered at 1 kHz.

Biochemistry. Expression of recombinant protein in bacteria and purification were carried out as described in refs. 15 and 47. Purified GST-fusion proteins were used for *in vitro* PIP_3 -binding assays in buffer containing 10 mM Hepes (pH 7.4), 150 mM NaCl, 5 mM EDTA and 0.25% Nonidet P-40. PIP_3 -agarose beads and the GST-Grp1PH positive-control protein were from Echelon Biosciences (Salt Lake City, UT). Fifty microliters of a 50% slurry of PIP_3 beads and purified protein (2 $\mu\text{g}/\text{ml}$) were incubated in 0.5 ml of binding buffer for 2 h at 4°C with rocking. Beads were gently pelleted and washed five times with excess binding buffer; PIP_3 -interacting proteins were eluted with $1\times$ NuPAGE sample buffer (Invitrogen). Protein samples then were separated under reducing conditions in 4–12% Bis-Tris gels and blotted onto nitrocellulose by using the NuPAGE transfer buffer system (Invitrogen). Blotted proteins were detected by using B-14 anti-GST monoclonal antibody (Santa Cruz Biotechnology, Santa Cruz, CA) at a dilution of 1:2,000 in 1% milk/500 mM

$\text{NaCl}/20$ mM Tris-HCl (pH 7.5)/0.05% Tween 20, HRP-conjugated anti-mouse IgG secondary antibody, and the Super-Signal West Dura Extended Duration chemiluminescence substrate (Pierce Biotechnology, Rockford, IL).

CaM-overlay assays were carried out essentially as described in ref. 47. After blotting, GST-fusion proteins were probed for 1 h at room temperature with recombinant FLAG-tagged CaM (at ≈ 50 nM) in 10 mM Hepes (pH 7.4)/150 mM NaCl/0.5% Nonidet P-40/0.5% BSA/2 mM NTA/170 μM CaCl_2 (10 μM free Ca^{2+}), either with or without prior and concomitant incubation with 100 μM PIP_3 . Bound CaM was visualized by using M2 anti-FLAG antibody (Sigma), and the CaM signal was quantified by using Kodak (New Haven, CT) 1D Image Analysis software. Blots subsequently were stripped and reprobed with an antibody against GST to ensure that equivalent amounts of fusion protein were blotted in all lanes. Control Western blots for CaM demonstrated that incubation with PIP_3 did not interfere with antibody binding or blot processing (data not shown). Inhibition of CaM binding is expressed as percentage reduction compared with control \pm SEM.

We thank Dr. Martin Biel (Ludwig-Maximilians University, Munich, Germany) for providing the DNA-encoding CNGA3, CNGA4, and CNGB1b and Dr. William Zagotta (University of Washington) for the DNA-encoding CNGA2 and the GST-fusion peptides. This work was supported by the National Institutes of Health (NIH) Ruth Kirchstein National Predoctoral Research Service Award NS052103 (to J.D.B.) and NIH Grants EY009275 (to J.W.K.), EY12836 (to M.D.V.), and EY12837 (to R.L.B.).

- Buck L, Axel R (1991) *Cell* 65:175–187.
- Ronnett GV, Moon C (2002) *Annu Rev Physiol* 64:189–222.
- Ache BW, Young JM (2005) *Neuron* 48:417–430.
- Axel R (2005) *Angew Chem Int Ed Engl* 44:6110–6127.
- Kaupp UB, Seifert R (2002) *Physiol Rev* 82:769–824.
- Kleene SJ (1993) *Neuron* 11:123–132.
- Kolesnikov SS, Kosolapov AV (1993) *Biochim Biophys Acta* 1150:63–72.
- Reisert J, Lai J, Yau KW, Bradley J (2005) *Neuron* 45:553–561.
- Bradley J, Reisert J, Frings S (2005) *Curr Opin Neurobiol* 15:343–349.
- Spehr M, Wetzel CH, Hatt H, Ache BW (2002) *Neuron* 33:731–739.
- Zhainazarov AB, Spehr M, Wetzel CH, Hatt H, Ache BW (2004) *J Membr Biol* 201:51–57.
- Chen TY, Yau K-W (1994) *Nature* 368:545–548.
- Liu M, Chen TY, Ahamed B, Li J, Yau K-W (1994) *Science* 266:1348–1354.
- O'Neil KT, DeGrado WF (1990) *Trends Biochem Sci* 15:59–64.
- Varnum MD, Zagotta WN (1997) *Science* 278:110–113.
- Trudeau MC, Zagotta WN (2003) *J Biol Chem* 278:18705–18708.
- Zheng J, Varnum MD, Zagotta WN (2003) *J Neurosci* 23:8167–8175.
- Sautter A, Zong X, Hofmann F, Biel M (1998) *Proc Natl Acad Sci USA* 95:4696–4701.
- Bonigk W, Bradley J, Muller F, Sesti F, Boekhoff I, Ronnett GV, Kaupp UB, Frings S (1999) *J Neurosci* 19:5332–5347.
- Zheng J, Zagotta WN (2004) *Neuron* 42:411–421.
- Bradley J, Bonigk W, Yau KW, Frings S (2004) *Nat Neurosci* 7:705–710.
- Gordon SE, Downing-Park J, Tam B, Zimmerman AL (1995) *Biophys J* 69:409–417.
- Crary JJ, Dean DM, Nguitragool W, Kurshan PT, Zimmerman AL (2000) *J Gen Physiol* 116:755–768.
- Dean DM, Nguitragool W, Miri A, McCabe SL, Zimmerman AL (2002) *Proc Natl Acad Sci USA* 99:8372–8377.
- Womack KB, Gordon SE, He F, Wensel TG, Lu CC, Hilgemann DW (2000) *J Neurosci* 20:2792–2799.
- Brady JD, Rich TC, Le X, Stafford K, Fowler CJ, Lynch L, Karpen JW, Brown RL, Martens JR (2004) *Mol Pharmacol* 65:503–511.
- Grunwald ME, Zhong H, Lai J, Yau K-W (1999) *Proc Natl Acad Sci USA* 96:13444–13449.
- Bradley J, Reuter D, Frings S (2001) *Science* 294:2176–2178.
- Munger SD, Lane AP, Zhong H, Leinders-Zufall T, Yau KW, Zufall F, Reed RR (2001) *Science* 294:2172–2175.
- Jenkins P, Hurd TW, Zhang L, McEwen DP, Brown RL, Margolis B, Verhey KJ, Martens JR (2006) *Curr Biol* 16:1211–1216.
- Oliver D, Lien CC, Soom M, Baukowitz T, Jonas P, Fakler B (2004) *Science* 304:265–270.
- Cukras CA, Jeliakzova I, Nichols CG (2002) *J Gen Physiol* 119:581–591.
- Huang CL, Feng S, Hilgemann DW (1998) *Nature* 391:803–806.
- Logothetis DE, Zhang H (1999) *J Physiol (London)* 520:630.
- Pochynuk O, Staruschenko A, Tong Q, Medina J, Stockand JD (2005) *J Biol Chem* 280:37565–37571.
- Tseng PH, Lin HP, Hu H, Wang C, Zhu MX, Chen CS (2004) *Biochemistry* 43:11701–11708.
- Dong K, Tang L, MacGregor GG, Hebert SC (2002) *J Biol Chem* 277:49366–49373.
- Zhang H, He C, Yan X, Mirshahi T, Logothetis DE (1999) *Nat Cell Biol* 1:183–188.
- Shyng SL, Cukras CA, Harwood J, Nichols CG (2000) *J Gen Physiol* 116:599–608.
- Prescott ED, Julius D (2003) *Science* 300:1284–1288.
- Ishii M, Inanobe A, Kurachi Y (2002) *Proc Natl Acad Sci USA* 99:4325–4330.
- McLaughlin S, Murray D (2005) *Nature* 438:605–611.
- Hegg CC, Greenwood D, Huang W, Han P, Lucero MT (2003) *J Neurosci* 23:8291–8301.
- Wang M, Kong Q, Gonzalez FA, Sun G, Erb L, Seye C, Weisman GA (2005) *J Neurochem* 95:630–640.
- Czajkowski R, Banachewicz W, Ilnytska O, Drobot LB, Baranska J (2004) *Br J Pharmacol* 141:497–507.
- Brown RL, Lynch LL, Haley TL, Arsanjani R (2003) *J Gen Physiol* 122:749–760.
- Peng C, Rich ED, Thor CA, Varnum MD (2003) *J Biol Chem* 278:24617–24623.